ACS chemical biology

ARTICLE

Metabolite Induction of *Caenorhabditis elegans* Dauer Larvae Arises via Transport in the Pharynx

Thomas J. Baiga[†], Haibing Guo[‡], Yalan Xing[‡], George A. O'Doherty[‡,*], Andrew Dillin[§], Michael B. Austin[†], Joseph P. Noel[†,*], and James J. La Clair[¶,*]

[†]Howard Hughes Medical Institute, Jack H. Skirball Center for Chemical Biology and Proteomics, The Salk Institute for Biological Studies, 10010 North Torrey Pines Road, La Jolla, California 92037, [‡]Department of Chemistry, West Virginia University, Morgantown, West Virginia 26506, [§]The Salk Institute for Biological Studies, Molecular and Cell Biology Laboratory, 10010 North Torrey Pines Road, La Jolla, California 92037, and [¶]Xenobe Research Institute, 3371 Adams Avenue, San Diego, California 92116

ABSTRACT *Caenorhabditis elegans* sense natural chemicals in their environment and use them as cues to regulate their development. This investigation probes the mechanism of sensory trafficking by evaluating the processing of fluorescent derivatives of natural products in *C. elegans*. Fluorescent analogs of daumone, an ascaroside, and apigenin were prepared by total synthesis and evaluated for their ability to induce entry into a nonaging dauer state. Fluorescent imaging detailed the uptake and localization of every labeled compound at each stage of the *C. elegans* life cycle. Comparative analyses against natural products that did not induce dauer indicated that dauer-triggering natural products accumulated in the cuticle of the pharnyx. Subsequent transport of these molecules to amphid neurons signaled entry into the dauer state. These studies provide cogent evidence supporting the roles of the glycosylated fatty acid daumone and related ascarosides and the ubiquitous plant flavone apigenin as chemical cues regulating *C. elegans* development.

*Corresponding authors,
i@xenobe.org,
noel@salk.edu,
george.odoherty@mail.wvu.edu.

Received for review December 26, 2007
and accepted March 7, 2008.

Published online April 1, 2008

10.1021/cb700269e CCC: $40.75

In nature, the multifaceted lifecycle of nematodes typically involves passage through multiple host–guest relations (*1*). While genomic and proteomic experiments provide a blueprint of an organism, they do not provide a complete explanation of the molecular communication between organisms and their environment. Environmental signals often trigger responses that are far more complex than those elicited by a single genetic or proteomic event (*2*). Within recent years, the discovery and elucidation of small molecule signals that induce *C. elegans* into a dauer or resting state has opened a new avenue for understanding how environmental cues regulate development and aging (*3*). In this investigation, we focus attention on the physiological mechanisms by which *C. elegans* sense and process fluorescent analogs of natural products. Our studies compare endogenous and xenobiotic signals with an attempt to identify the molecular plasticity of the *C. elegans* lifecycle.

C. elegans sense environmental signals in part through ciliated amphids at the tips of their heads and phasmids in their tails (*4–6*). Early tracking experiments established that fluorescent dyes such as fluorescein isothiocyanate (FITC) move from solution through the cilia at the top of their heads to sensory neurons within the amphid (*7*). While genetic approaches have uncovered aspects of the signal transduction pathways involved in this reception (*8–10*), the underlying mechanisms by which the chemical signals are transported and processed within *C. elegans* remain unresolved.

Small molecules, including damone (**1**), trigger the entry of L1 larvae into a nonaging dauer state. Recently, the structure of **1** was determined by isolation from large scale extracts of *C. elegans* followed by a combina-

tion of NMR studies (*11*) and total syntheses (*11, 12*). Using this molecule as a starting point, we investigated the transport of **1** and other non-dauer-inducing natural products in *C. elegans*. The goal of these studies was to identify and visualize features underlying the mechanism or mechanisms by which **1** enters the worm. In particular, we hoped to determine whether this transport was related to dauer induction or was a general phenomenon of small molecule uptake and transit. If mechanisms underlying uptake of **1** were specific to dauer induction, we then sought to address whether other natural products found in the environmental niche of *C. elegans* could also access components of the discovered transport mechanisms.

RESULTS AND DISCUSSION

Our studies began with the preparation of a panel of molecular probes (Schemes 1 and 2). This effort was streamlined by using a centralized method to prepare a group of labeled natural products, each bearing a single common fluorophore (*12*). The use of a single dye not only was advantageous to expedite our synthetic efforts but also allowed us to directly compare each labeled natural product with minimal spurious perturbations.

Synthesis of Fluorescent Probes 4 and 5 from Daumone 1. Our studies began by evaluating daumone **1**, a signal for dauer stage entry (*2, 11*). Using an approach recently developed by O'Doherty (*13*), we prepared 100 mg of daumone (**1**) by total synthesis. Aliquots of this material were then coupled in parallel to blue and green fluorescent amines **2** (see ref 12) and **3** (*14*) by treatment with *O*-benzotriazole-*N*,*N*,*N*′,*N*′-tetramethyl-uronium-hexafluoro-phosphate (HBTU; Scheme 1) to deliver **4** and **5**, respectively. Complete synthetic details are provided within the Supporting Information.

We then screened **4** and **5** for their ability to mimic **1** *in vivo*. We began by determining the activity of **1**, **4**, and **5** in *C. elegans* using agar plates (see ref 11). After these assays were conducted, it became apparent that the solubility of **1**, **4**, and **5** in agar led to the formation of gradients of **1**, **4**, and **5** within the gel. These gradients were readily apparent upon examination of the fluorescence from **4** or **5** in cross-sections of the each gel, either using a CCD camera or employing a fluorescent microscope. While liquid agar was amenable to the addition of **4** or **5**, we often found that during cooling a considerable portion of the probes concentrated in the aqueous media surrounding the gel. The presence of these gradients was problematic when screening for dauer induction, because the movement of worms through the plate would uncontrollably adjust their exposure to compound and thereby increase the likelihood of inducing secondary effects such as chemotactic responses (*15*).

On the basis of this concern, we developed a liquid based assay that provided a homogeneous solution of **1**, **4**, and **5** (Figure 1). When this screen was used, worms entered dauer development (Figure 1, panel a) when treated with **1** at an ED_{50} value of 50 ± 10 μM (Figure 1, panels b and c). This value was considerably lower than the 386 μM (see ref 11) reported using agar analyses (*16*). The blue fluorescent analog **4** was slightly more active and the green fluorescent analog **5** less active than **1** with ED_{50} values of 20 ± 5 μM and 200 ± 25 μM, respectively.

Fluorescent Probes 4 and 5 Localize within the Pharyngeal Cuticle of Adult *C. elegans*. We next evaluated the localization of **4** and **5** in live adult *C. elegans*. Worms were treated with a mixture of **4** and **5** and then gauged by two-color image analysis (Figure 2, panel a). While comparable in localization, the fluorescence from **4** (Figure 2, panel b) or **5** (Figure 2, panel c) did not appear in the amphid neurons but rather concentrated within the cuticle of the pharynx and in the first intestinal cell, Int1, in adult animals. Control experiments were conducted to establish that fluorescent labeling did not alter probe uptake. First, we established that fluorescent dye **12** was readily removed, returning worms that were indistinguishable from those treated with solvent alone (Figure 2, panel d). Only autofluorescent cells appeared when worms were imaged after compound **12** was cleared from their intestinal track (Figure 2, panel e). Second, we determined that 100 μM **1** completely inhibited the uptake of 5 μM **4** or **5**, thereby verifying that **4** and **5** shared their uptake machinery with **1**.

Daumone 1 Is Not the Only Natural Product That Can Induce Dauer Development. Initially, we were interested in determining whether the localization of **4** and **5** in the cuticle of the pharynx (Figure 2, panels b and c) was a general phenomenon observed during natural product digestion or the response was specific to materials that induced entry into dauer development. We addressed this question by screening a small library of natural products ($N = 953$) for inducers of dauer development. Again, we found that a liquid based screen was far more effective because it could be conducted rap-

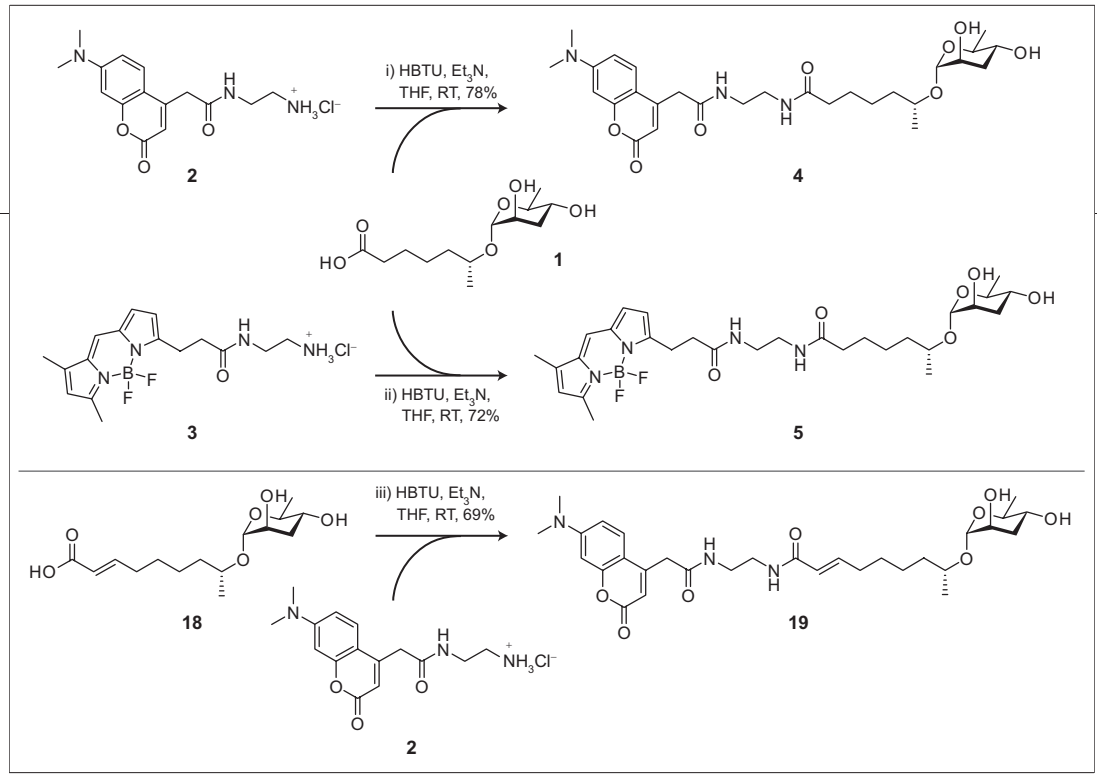

Scheme 1. Structures and syntheses of fluorescent probes 4 **and** 5 **from daumone** 1 **and** 19 **from ascaroside** 18**.**

idly with reduced effort. From this screen, only apigenin **14** induced dauer formation at a concentration under 100 μM; the bulk of the natural products either resulted in no response or were toxic.

The identification of apigenin **14** was not completely surprising because recent studies by Shim and coworkers (*17*) indicate that **14** inhibited the growth of *C. elegans*. In their studies, L1 stage worms treated with **14** reached L4 stage with only modest growth inhibition. However, potent growth inhibition was observed in progeny of worms treated with **14**. Intrigued by these observations, we prepared a fluorescent analog of apigenin **13** for comparison with **4** and **5**.

After evaluation of several synthetic schemes (*18*), an optimum route was established beginning with the protection of 2,4,6-trihydroxyacetophenone **6** as its bis-methoxyethoxymethyl (MEM) ether **7** (Scheme 2). Once protected, an aldol condensation with *p*-alloxybenzaldehyde **8** was used to provide chalcone **9**. Subsequent ring closure of **9** in the presence of I_2 afforded 4′-alloxyapigenin **10**. Fluorescent analog **13** was prepared by applying olefin cross metathesis with Grubbs second-generation catalyst **11** to couple **10** to **12** (see ref 13). Complete synthetic details are provided within the Supporting Information. We then evaluated the activity of **13** (Scheme 2). Liquid phase screening (Figure 1) indicated that the fluorescent apigenin analog **13** also induced dauer formation with an ED_{50} value of 80 ± 20 μM. However, this activity was accompanied by considerable toxicity as indicated by an LD_{50} value of 50 ± 10 μM.

Comparable labeling methods were also used to prepare fluorescent analogs of natural products identified as toxic (LD_{50} value < 100 μM) during the library screening effort. Mycophenolic acid and amphotericin B were selected given ready access to active fluorescent analogs. Using the methods in Scheme 2, we synthesized the first toxic probe **16** by coupling mycophenolic acid **15** to **2**. An amphotericin B analog **17** was also prepared using previously described methods (see ref 14). The toxicity of these analogs was validated by toxicity screening (*19*) in wild-type *C. elegans* returning LD_{50} values of 90 ± 10 μM for **16** and 110 ± 20 μM for **17**. Subsequent screening indicated that neither **16** nor **17** induced dauer development.

We then compared the localization of the apigenin probe **13** and the two toxic probes, **16** and **17**, against the fluorescent daumone probes **4** and **5** (Figure 2, panels a–c). While more diffuse than **4**, apigenin **13** also localized within the buccal cavity cuticle, procorpus, pharyngeal sieve, isthmus, and grinder of the pharynx (Figure 2, panel f). The two toxic materials **16** (Figure 2, panel g) and **17** (Figure 2, panel h), however, localized in a different fashion, appearing throughout the worm with slight concentration in the gonad and basal membrane of the pharynx.

Development of Fluorescent Probes with Enhanced Dauer Activity Permits *in Vivo* Imaging of Neuronal Transmission. As these studies were completed, Schroeder and Clardy reported the isolation of ascaroside **18** (Scheme 2) from extracts of *C. elegans* (*20*). Activity analyses indicated that ascaroside **18** was 2 or-

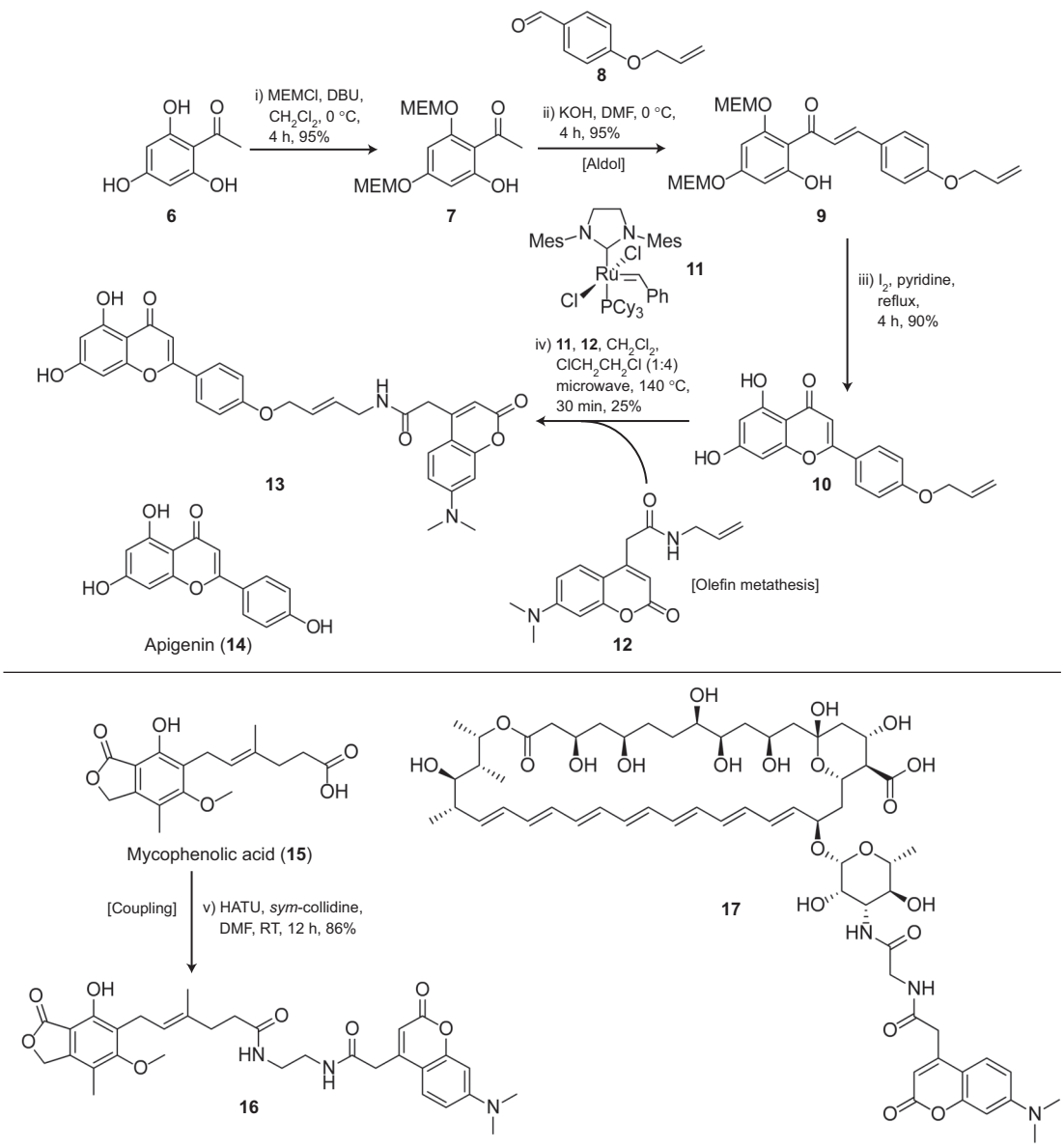

Scheme 2. Structures and syntheses of fluorescent probes 13 **from apigenin** 14**,** 16 **from mycophenolic acid** 15**, and amphotericin probe** 17**.**

ders of magnitude more potent than **1**. The question then remained as to whether **1** and **18** were processed by the same mechanism within the worm. Intrigued by this query, we synthesized **18** by means of our *de novo* asymmetric synthesis (see ref 12) and coupled it to dye **2** by treatment with *o*-(7-azabenzotriazol-1-yl)-*N*,*N*,*N*′,*N*′-tetramethyluronium hexafluorophosphate (HATU) and *sym*-collidine in DMF to produce probe **19** (Scheme 2). We then determined that ascaroside **18** and its fluorescent analog **19** induced dauer with EC_{50} values of 1.6 and 2.1 μM, respectively, when worms were treated during L1 (Figure 1, panels b and c). These values are in agreement with the published EC_{50} value of 1.1 μM for **18** (see ref 20).

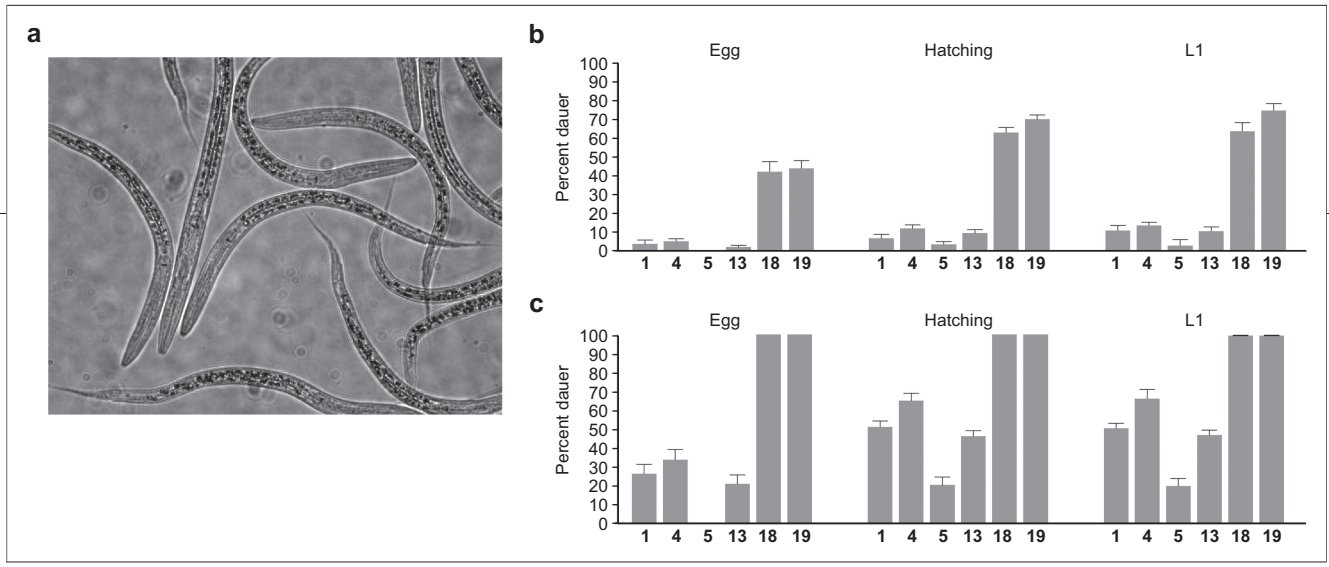

Figure 1. Screening for dauer induction. a) A white light image depicting *C. elegans* induced into dauer state by 4. Relative activity of dauer-inducing probes at b) 1 μM or c) 50 μM. Assays were developed by treating 200−300 worms as egg, during hatching, or in L1 stage with the ascribed compound in a volume of 200 μL of M9 media for 20 min. The worms were then washed with fresh media to clear unabsorbed probes, transferred to blank NG agar plates, and incubated for 52−72 h at 23 °C. The percentage of dauer worms was determined from the average of five assays of 200−300 worms. Each screen was conducted with a solvent control at 0−2% dauer formation. Dauer states were counted in agar based upon their characteristic morphology as apparent in panel a and verified by counting the worms after treatment with 1% (w/v) aqueous SDS solution. The average and deviation of both plate and SDS-treated larvae are presented.

To ensure complete validation of this analysis, we carefully screened a temporal window of natural product exposure beginning at egg stage and running until L2. As shown in Figure 1, only minor deviations were observed if the worms were treated at the beginning or end of L1 stage. However, we noticed that the efficacy of **18** or **19** also dropped when they were added during egg stage (~30% reduction). Comparable observations were obtained with **1**, **4**, and **13** (Figure 1, panel c).

We then compared the activity of **19** with that of **5** using two-color image analysis. A 200-fold excess of **5** to **19** was required to obtain comparable emission. After exposure of adult worms for 1 h, both **5** and **19** were observed within the buccal cavity cuticle, procorpus, pharyngeal sieve, isthmus, and grinder of the pharynx (Figure 2, panel i). However, the more active ascaroside **19** was also observed within an amphid intermediate neuron (AIN) on the right side of the Int1 cell.

We continued these studies by conducting time course imaging to identify other neurons that were targeted by compound **19**. Within 10 min of exposure, ascaroside **19** was observed in neurons at the anterior of the terminal bulb of the pharynx (Figure 2, panel j). Unfortunately after screening concentration, time, and fixation methods, we were not able to obtain sufficient resolution to assign the localization to a single neuron. We were also not able to resolve these cells using confocal or two-photon microscopy. This lack of resolution suggested that **19** moved between several neurons within this region. By analysis of the image in Figure 2, panel j, one can see multiple regions of intensity for both left and right axes. This observation makes anatomical sense because the neurons shown to be involved in activating dauer state, ADF, ASG, ASI, and ASJ, are found within these bilaterally symmetric areas. In addition, attempts at identifying the position of these neurons by costaining with fluorescent dyes (i.e., DIL) also lacked resolution suggesting that the activity of **19** somehow altered the transport of DIL as compared with that in untreated wild-type organisms (not shown). Further, attempts to identify the position of the neurons by comparison with differential interference contrast (DIC) phase contrast images was also complicated due the diffuse nature of the fluorescent region about the amphid neurons (AN in Figure 2, panel j). While correlation between the more active analog **19** appearing in amphid neurons and pharynx and the less active **4** and **5** appearing only in the pharynx was suggestive that the more extensive localization of analog **19** was related to additional sensory transitions; the inability to obtain higher resolution prevented us from providing a complete description of the neuronal transport of **19**.

We then validated that **1** and **18** share common targets by conducting competition experiments. The treatment of adult worms with **18** blocked the subsequent uptake of both **4** (Figure 2, panel k) and **19** (Figure 2, panel l) indicating that these materials did in fact share a common mechanism of initial localization. Comparable experiments were conducted on daumone **1** and apigenin **14**. While complicated by solubility issues, 5 μM apigenin **14** reduced the uptake in the pharynx of 1 μM **13** or 1 μM **5** by 25% ± 5% or 32% ± 6%, respectively. These values were obtained by comparing the average fluorescence intensity observed in the phar-

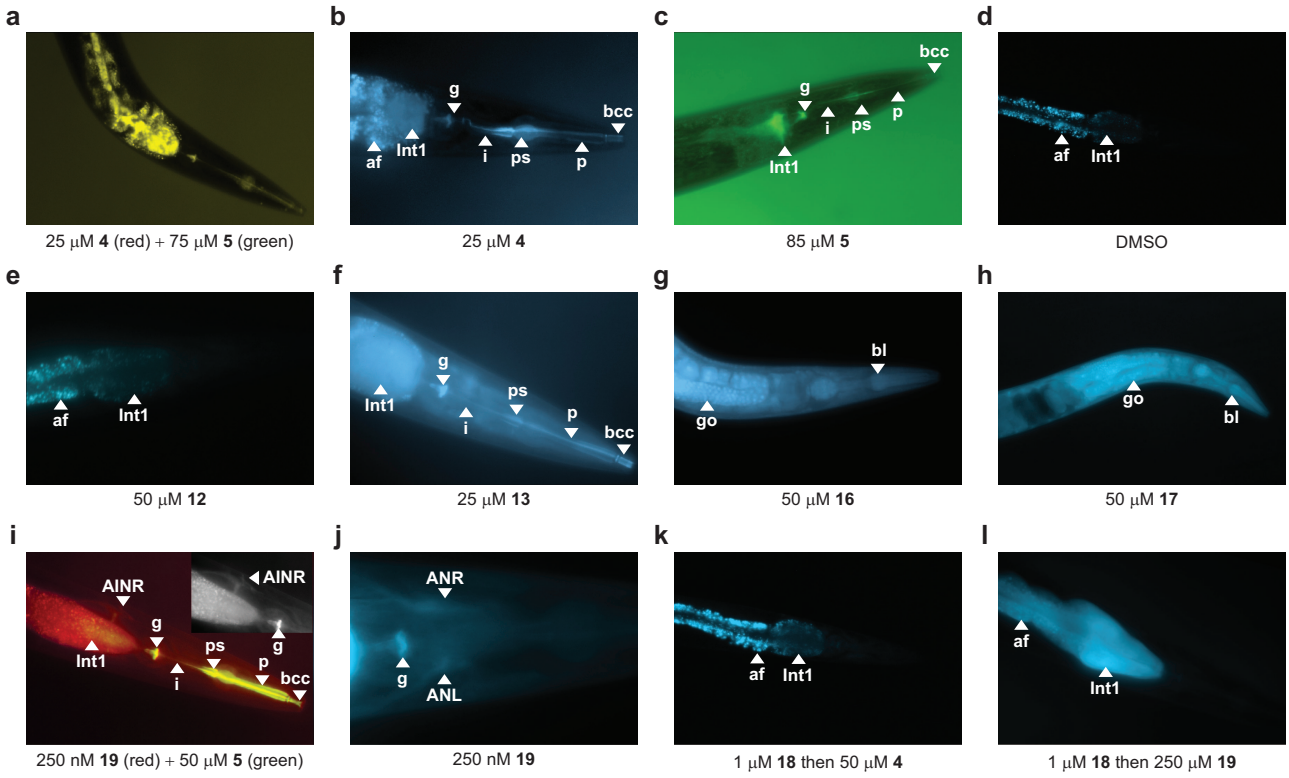

Figure 2. Histological localization of fluorescent natural product analogs in live wild-type adult *C. elegans* variety Bristol strain N2. a) Daumone analogs 4 (red) and 5 (green) colocalize in adult *C. elegans* as given by appearance of yellow from the mixing of red and green. Both b) 4 and c) 5 concentrated within buccal cavity cuticle (bcc), procorpus (p), isthmus (i), pharyngeal sieve (ps), and grinder (g) of the cuticle of the pharynx and the first intestinal cell (Int1). Control experiments as given by the treatment of adult worms with d) solvent or e) compound 12 followed by washing with media returned worms with only autofluorescent cells within the gut (af) and the first intestinal cell (Int1). f) Apigenin analog 13 also localizes within the cuticle of the pharynx (bcc, p, ps, i, and g) and the first intestinal cell (Int1). g) The two toxic probes 16 and 17 do not target the cuticle of the pharynx with uptake apparent throughout the majority of the worm and modest concentration within the gonad (go) and basal lamina (bl) of the pharynx. h) The localization of amphotericin analog 17 was comparable to that of 16 bearing a similar dispersion throughout the worm and modest concentration in the gonad (go) and basal lamina (bl) of the pharynx. i) Blue fluorescent 19 (false colored in red) and green fluorescent daumone 5 (in green) colocalize within the cuticle of the pharynx. The more active ascaroside 19 is also observed in an amphid intermediate neuron (AINR) on the right side of the worm. j) When treated for a shorter period of 10 min, ascaroside 19 is observed within both right and left amphid neurons (ANR and ANL) near the posterior to the terminal bulb of pharynx and grinder (g). Pretreatment of worms with 18 blocks the uptake of both k) 5 and l) 19. Images were collected after treating adult worms with ascribed compound in M9 media for 1 h and were then washing with M9 media to clear each probe from the digestive track, unless noted otherwise. Blue fluorescence was collected by excitation at 377 ± 50 nm and emission at 447 ± 60 nm. Green fluorescence was collected by excitation at 500 ± 24 nm and emission at 542 ± 27 nm.

ynx in images of worms (35−50 worms used per data point) that were pretreated with **14** to that in images of untreated worms.

Life Cycle Analyses Support the Metabolite Interplay between Neuronal and Pharyngeal Structures. Because of the lack of resolution of the neuronal uptake of **19**, we turned our attention to examining the transport of these molecules through the more relevant dauer states (note that adult hermaphrodites have passed the window to enter dauer state). Initially, our goal was to develop a detailed temporal and spatial picture of the transport of the dauer-inducing probes as L1 worms entered the dauer state. After beginning our analyses, we soon realized that the transport of the fluorescent dauer probes **4**, **5**, **13**, and **19** was far more complex than that arising from examining a single state change. We therefore expanded the scope of our study to examine the trans-

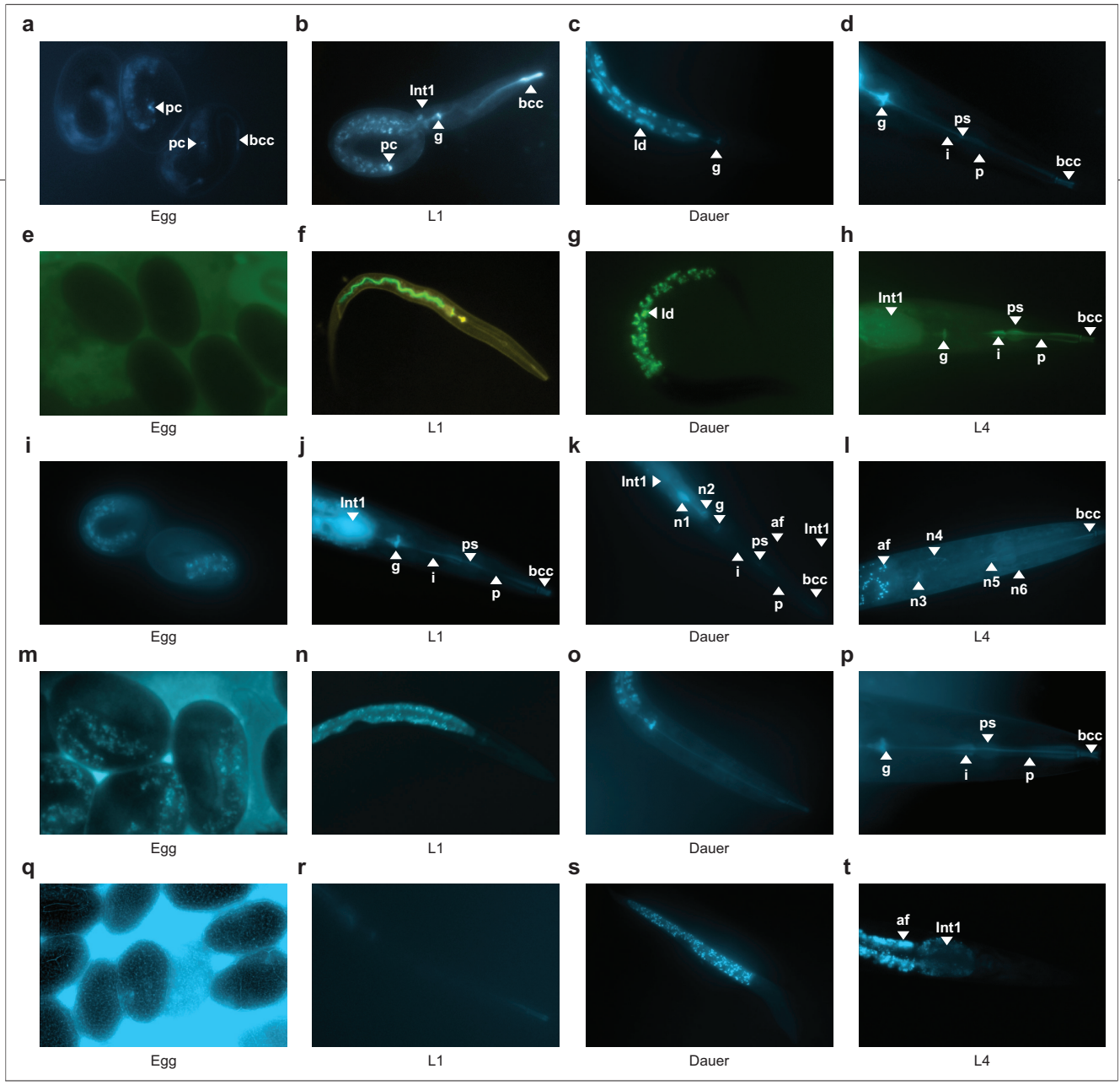

Figure 3. Life cycle analysis. a) Embryos treated with 25 μM 4 in M9 media. b) A worm hatching after being treated with 25 μM 4 in M9 media during embryogenesis. This worm grows into c) a dauer worm and exits dauer as d) an L4 worm. e) Embryos treated with 50 μM 5 in M9 media. f) A worm hatched in 50 μM 5 in M9 media after being treated during embryogenesis with 25 μM 4 in M9 media. This worm grows into g) a dauer state and exits dauer as h) an L4 worm. i) Embryos treated with 50 μM 13 in M9 media. j) A worm treated with 50 μM 13 in M9 in L1 progresses into k) a dauer state and exits as l) an L4 worm. m) Embryos treated with 10 μM 19 in M9 media. n) A worm treated with 10 μM 19 in M9 in L1 enters into o) a dauer state and exits as p) anL4 worm. q) Embryos treated with 50 μM control 12 in M9 media. r) A worm treated with 50 μM of control 12 in M9 in L1 enters into s) a dauer state and exits as t) an L4 worm. Unless otherwise noted, the worm in panels b—d, f—g, j—l, n—o, and r—t were treated at L1 with the ascribed compound in M9 media, washed three times with an equivalent volume of M9 media, and then transported to M9 agar for entry into the dauer state and subsequent return to L4. Blue fluorescence was collected by excitation at 377 ± 50 nm and emission at 447 ± 60 nm, and green was collected by excitation at 500 ± 24 nm and emission at 542 ± 27 nm. Abbreviations: af, autofluorescent gut cells; bcc, buccal cavity cuticle; g, grinder; i, isthmus; Int1, first intestinal cell; ld, lipid droplets; n1—n6, neurons; p, procorpus; ps, pharyngeal sieve; pc, posterior cell.

port phenomena from the egg to dauer states followed by their re-entry as L4 larvae and growth into adult hermaphrodites.

Using eggs collected from adult hermaphrodites, we observed that blue fluorescent probes **4** (Figure 3, panel a), **13** (Figure 3, panel m), and **19** (Figure 3, panel i) were readily apparent in developing larvae within the eggs, while the green fluorescent **5** (Figure 3, panel e) and control **12** (Figure 3, panel q) were not. Surprisingly, this uptake was targeted to specific cells within the anterior of the developing embryo. After treatment at the egg stage with **4**, fluorescence was also ob-

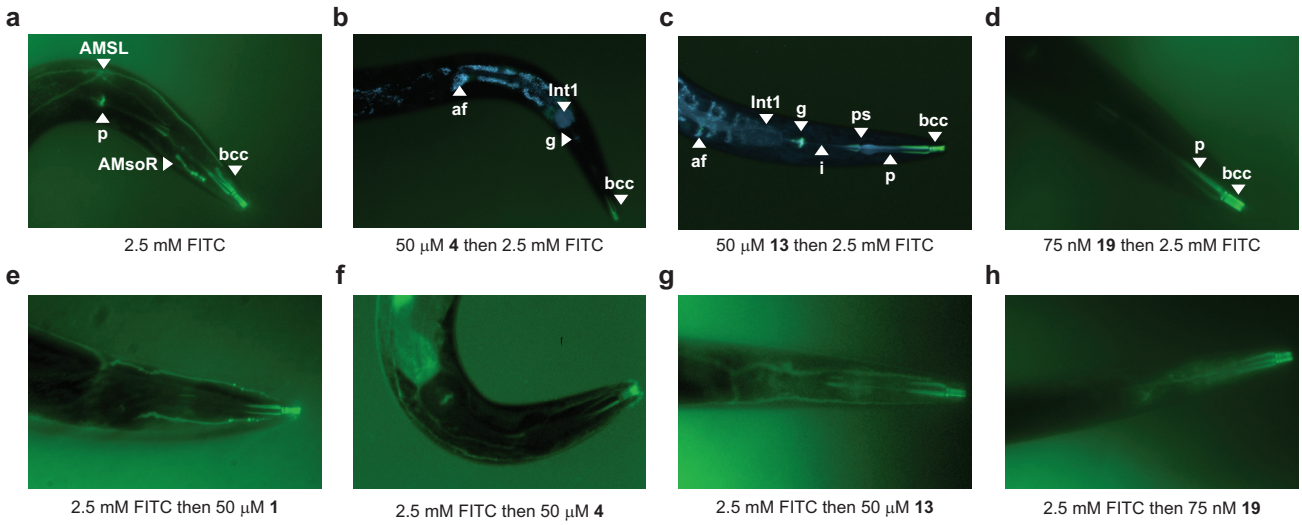

Figure 4. Dauer-inducing natural products block the staining of amphid neurons. a) The uptake of FITC in an adult hermaphrodite. Two-color images indicate that treatment of worms with b) 4**, c)** 13**, or d)** 19 **blocks the uptake of FITC. Worms treated first with FITC and then with e)** 1**, f)** 4**, g)** 13**, or h)** 19 **are not capable of expelling FITC from their amphid neurons. Blue fluorescence was collected by excitation at 377 ± 50 nm and emission at 447 ± 60 nm, and green was collected by excitation at 500 ± 24 nm and emission at 542 ± 27 nm.**

served during hatching in the pharynx and in specific cells at the posterior (pc) of the worm (Figure 3, panel b). Comparable localization within these cells was also observed when worms were treated with **13** and **19**. These posterior cells remained fluorescent only for a brief time after hatching, as the L1 worms that developed after treatment with **4** during embryogenesis (Figure 3, panel f) no longer displayed fluorescence in these cells.

We also determined that probe localization in L1 worms that were treated during embryogenesis was identical to that in worms treated after entry into L1 stage using two-color analysis. Embryos were treated with blue fluorescent **4** until just prior to hatching, washed three times with media, and transferred into media containing **5** (Figure 3, panel f). Because **5** was shown not to cross into the egg (Figure 3, panel e), the presence of green fluorescence in hatched worms was suggestive of uptake after hatching, and blue fluorescence was indicative of uptake during the egg stage. Other than the obvious enhancement of **5** in the intestinal track, the localization of **4** and **5** fluorescence as given by the formation of yellow (Figure 3, panel f) was identical, thereby confirming that comparable uptake occurred prior to and after hatching.

Next, we tracked the localization of probes as worms transitioned into the dauer diapause. At the completion of L1, worms failed to cross into the L2 stage as **4**, **5**, **13**, and **19** induced diapause. After reaching the dauer state, fluorescence from **4**, **5**, and **13** appeared in lipid droplets (as assigned by comparison with DIC microscopy) within the intestine in worms treated with **4** (Figure 1, panel c), **5** (Figure 3, panel k), **13** (Figure 3, panel o), and **19** (not shown). The position of these lipid droplets can also be compared with the autofluorescent cells in control **12** (Figure 3, panel s). The more active **19**, however, also resulted in significant localization in the cuticle of the pharynx and in neurons posterior to the grinder (n1 and n2 in Figure 3, panel k). Similar localization of the apigenin analog **13** was also observed in the pharyngeal cuticle (Figure 3, panel o).

We then evaluated worms as they exited the dauer diapause. Because the worms were treated with the corresponding probe prior to entry into the dauer stage, any fluorescence observed at this stage arose from probe that was previously acquired and stored throughout the dauer process. Remarkably, fluorescence from **4** (Figure 3, panel d), **5** (Figure 3, panel h), and **13** (Figure 3, panel l) was retained in the cuticle of the pharynx after exit from the dauer state. This observation

was in agreement with the localization of these probes when presented to L4 stage worms (not shown) or during the adult stage (Figure 2). The localization of the more potent analog **19** also appeared within neurons (n3−n6 in Figure 3, panel l) of the L4 stage worm. While the function and role of this response is not understood at this time, the suggestion that worms also sense their internally stored natural products well after exit from the dauer state may be indicative of a unique mechanism of transit and secondary signaling.

Blockage of Neuronal Dye Uptake. Intrigued by this observation, we returned to adults to evaluate the role that the dauer-inducing probes played in regulating neuronal sensing. We applied the Hedgecock staining method (*22*) to address the lack of localization of **4**, **5**, and **13** within amphid neurons (see also ref 8). In this method, fluorescein isothiocyanate (FITC) stains six pairs of amphid sensory neurons (Figure 4, panel a). Strikingly, the addition of **1**, **4**, **5**, **13**, **14**, **18**, and **19** blocked the uptake of FITC into the amphid neurons in a dose-dependent manner. From two-color imaging, the addition of **4** (Figure 4, panel b), **13** (Figure 4, panel c), or **19** (Figure 4, panel d) caused marked restriction of FITC to the buccal cavity cuticle. This was accompanied by substantial decreases in the localization of **4** and **13** in the pharyngeal sieve, grinder, and isthmus when compared with worms treated with FITC alone (Figure 4, panel a). The fact that **4** and **13** were not observed in the buccal cavity cuticle suggests that interactions in the pharyngeal cuticle regulate FITC uptake.

We then investigated the role of the probes in flushing FITC from the neurons. Worms were first treated with FITC and then probes **1** (Figure 4, panel e), **4** (Figure 4, panel f), **13** (Figure 4, panel f), and **19** (Figure 4, panel e) failed to clear FITC from amphid neurons. Together, these observations indicate that the blockage in FITC uptake arose from events triggered by the uptake of a dauer-inducing natural product. This suggestion is not a new observation (see ref 8), as occlusion has been noted in number of dauer-defective mutants including *daf-6*, *daf-10*, and *daf-19* (*21*–*23*). While we have yet to define a direct connection between the uptake of dauer-inducing natural products, contact with their receptors, and subsequent signal transduction networks, the FITC uptake blocking experiments demonstrate that **4**, **5**, **13**, and **19** generate responses common to genetic phenotypes.

To summarize, we have shown that daumone **1** and the corresponding fluorescent analogs **4** and **5** induce dauer formation. Similar activity was also observed for apigenin **14** and a fluorescent apigenin analog **15**. We also confirmed that the recently identified ascaroside **18** is considerably more active than daumone (**1**) and have prepared a more active fluorescent analog **19** thereof.

Histological analyses in live *C. elegans* indicate that daumone (**1**), apigenin (**13**), and ascaroside **18** concentrate in the cuticle of the pharynx in worms prior to dauer entry and in adults. This localized material is then transited to amphid neurons as a signal for dauer entry. The imaging of the latter process was only possible for the more active probe **19**. Life cycle studies indicate that **19** is stored in lipid cells during the dauer state and released into the cuticle and amphid neurons upon exit into the L4 stage. Moreover, we also observed that several of the dauer-inducing materials (e.g., **4**, **13**, and **19**) were able to cross the egg membrane and enter developing larvae. This transport event was also effective in leading subsequent worms into dauer development. This transition occurred both before and after egg laying suggesting that dauer induction can be communicated from adults to their progeny. While further studies are needed to complete a detailed understanding of the mechanisms regarding the targeting of dauer-inducing probes during embryogenesis, the fact that shared localization of **4**, **13**, and **19** was observed in specific cells within the head of the embryo suggests that these materials also serve as developmental regulators.

In addition, the phenotypic mimicry of the plant-derived flavone **13** and its associated fluorescent probe **14** hints at other yet to be identified dauer-inducing molecules in the environmental niche of *C. elegans*. Moreover, the likely role of these natural compounds in mediating complex interspecies ecological interactions suggests the probable existence of intricate evolutionary processes affecting the tuning of biosynthesis in one species and signaling in another. In the specific laboratory setting examined here, the two classes of dauer-inducing natural products studied, ascarosides **4** and **19** and flavone **13**, were taken up and processed in a similar manner within the worm, while other non-dauer-inducing natural products such as **16** and **17** were taken up and localized using different mechanisms. These comparative observations suggest that a unique process exists for

dauer entry that involves absorption in the cuticle of the pharynx followed by transit to amphid neurons. Studies are now underway to link these images to subsequent physiological events leading to receptor modulation. In particular, current foci seek to understand why the lack of neuronal transfer (FITC uptake) occurs both in dauer-defective mutants and worms already induced by small molecules to enter the dauer state.

METHODS

General Synthetic Methods. Synthetic procedures and copies of NMR spectra for each material described are provided within the Supporting Information.

***C. elegans* Protocols.** *C. elegans* Bristol variety, strain N2, were grown on nematode growth media (NGM) agar plates with *E. coli* (OP50) as a food source under standard uncrowded and well-fed conditions at 20 °C unless otherwise stated.

Dauer Formation Assays. Adult worms were placed on a plate containing 3 mL of NGM agar and incubated at 20 °C for 4−6 h. After incubation, adult worms were removed, and the eggs or L1-staged progeny were collected by centrifugation after suspension of the agar in 5 mL of M9 media. Eggs or L1 stage worms were then resuspended in 190 μL of M9 media in a 96 well plate and treated with a 10 μL solution of the desired compound (**1**, **4**, **5**, **14**, or **15**) suspended in 50% (v/v) aqueous DMSO or 50% (v/v) aqueous ethanol. After incubation for 4 h at 23 °C, the solution was transferred to a 1 mL NGM agar plate, and the eggs or L1-stage larvae were then incubated for 52−72 h at 23 °C. The number of eggs or larvae was counted before and after incubation. A 1% (w/v) aqueous SDS solution (1.0 mL) was added to the plate, and the surviving worms were counted as dauer larvae.

Uptake Studies. Worms were gathered from plates by soaking 3 mL of agar in 10 mL of M9 media. Worms were collected by settling or by centrifugation at 1200 rpm (~450*g* force) for 2−3 min. In a 96 well plate, ~250 worms in 200 μL of M9 media were treated with a 20× solution of the fluorescent materials described in Figures 1 and 2 dissolved in 20−50% (v/v) aqueous DMSO. After incubation for 1 h, the solution was diluted into a tube containing 1 mL of chilled M9 media and incubated for 20 min. The worms were collected by centrifugation, the media was removed, and the process was repeated three times to clear materials from the intestine. Worms were immobilized by the addition of 0.5 M NaN_3 and mounted on a glass slide. Images were collected on a Nikon TE2000 microscope. Blue fluorescence was collected by excitation at 377 ± 50 nm and emission 447 ± 60 nm. Green fluorescence was collected by excitation at 500 ± 24 nm and emission 542 ± 27 nm. Red fluorescence was collected by excitation at 543 ± 22 nm and emission at 593 ± 40 nm. Images were accrued in grayscale and colored during subsequent image processing with Photoshop (Adobe) or ImageJ (NIH) (*24*).

FITC Uptake Studies. Worms were gathered from plates by soaking 3 mL of agar in 10 mL of M9 media. Worms were collected by settling or by centrifugation at 1200 rpm (~450*g* force) for 2−3 min. In a 96 well plate, ~250 worms in 200 μL of M9 media were treated with 10 μL of 500 μM **1**, **4**, **5**, or **13** in 50% (v/v) aqueous DMSO. Due to insolubility problems, treatment with **14** required a lower concentration by treatment of 200−300 worms in 20 μL of M9 media with 190 μL of 5 μM **14** in 10% (v/v) aqueous DMSO. After incubation for 1 h, 20 μL of a 25 mM solution of FITC in water was added. The worms were incubated for 4 h and then immobilized by the addition of 0.5 M NaN_3, mounted on a glass slide, and imaged. Images were collected on a Nikon TE2000 microscope. Blue fluorescence was collected by excitation at 377 ± 50 nm and emission 447 ± 60 nm. Green fluorescence was collected by excitation at 500 ± 24 nm and emission 542 ± 27 nm. Images were accrued in grayscale and colored during subsequent image processing.

Acknowledgment: We sincerely thank R. Aroian (University of California, San Diego) for provision of *C. elegans* and are grateful for suggestions provided by L. Avery (University of Texas Southwestern Medical Center), M. D. Burkart (University of California, San Diego), and D. Riddle (University of British Columbia). G.A.O. thanks the WVU ARTS Foundation, NIH (Grant GM63150), and NSF (Grant CHE-0415469). J.P.N. thanks NSF (Grant MCB-0236027) and the Howard Hughes Medical Institute.

Note Added after ASAP Publication. There were errors in Scheme 1 and Figure 1 of the version published ASAP April 1, 2008; the corrected version was published May 16, 2008.

Supporting Information Available: This material is free of charge *via* the Internet.

REFERENCES

1. Lee, D. L. (2002) *The Biology of Nematodes* (Lee, D. L., Ed.) 1st ed., pp 61−73, Taylor & Francis, New York.
2. Moran, N. A. (2006) Symbiosis, *Curr. Biol. 16*, R866–R871.
3. Lindblom, T. H., and Dodd, A. K. (2006) Xenobiotic detoxification in the nematode *Caenorhabditis elegans*, *J. Exp. Zool. A 305*, 720–730.
4. Golden, J. W., and Riddle, D. L. (1982) A pheromone influences larval development in the nematode *Caenorhabditis elegans*, *Science 218*, 578–580.
5. Larsen, P. L., Albert, P. S., and Riddle, D. L. (1995) Genes that regulate both development and longevity in *Caenorhabditis elegans*, *Genetics 139*, 1567–1583.
6. Wang, Y., and Levy, D. E. (2006) *C. elegans* STAT cooperates with DAF-7/TGF-beta signaling to repress dauer formation, *Curr. Biol. 16*, 89–94.
7. Hedgecock, E. M., Culotti, J. G., Thomson, J. N., and Perkins, L. A. (1985) Axonal guidance mutants of *Caenorhabditis elegans* identified by filling sensory neurons with fluorescein dyes, *Dev. Biol. 111*, 158–170.
8. Schroeder, F. C. (2006) Small molecule signaling in *Caenorhabditis elegans*, *ACS Chem. Biol. 1*, 198–200.
9. Burnell, A. M., Houthoofd, K., O'Hanlon, K., and Vanfleteren, J. R. (2005) Alternate metabolism during the dauer stage of the nematode *Caenorhabditis elegans*, *Exp. Gerontol. 40*, 850−856.
10. Fitch, D. H. (2005) Evolution: an ecological context for *C. elegans*, *Curr. Biol. 15*, R655−R658.
11. Jeong, P. Y., Jung, M., Yim, Y. H., Kim, H., Park, M., Hong, E., Lee, W., Kim, Y. H., Kim, K., and Paik, Y. K. (2005) Chemical structure and biological activity of the *Caenorhabditis elegans* dauer-inducing pheromone, *Nature 3433*, 541–545.
12. Alexander, M. D., Burkart, M. D., Leonard, M. S., Portonovo, P., Liang, B., Ding, X., Joullie, M. M., Gulledge, B. M., Aggen, J. B., Chamberlin, A. R., Sandler, J., Fenical, W., Cui, J., Gharpure, S. J., Polosukhin, A., Zhang, H. R., Evans, P. A., Richardson, A. D., Harper, M. K., Ireland, C. M., Vong, B. G., Brady, T. P., Theodorakis, E. A., and La Clair, J. J. (2006) A central strategy for converting natural products into fluorescent probes, *ChemBioChem 7*, 409−416.

13. Guo, H., and O'Doherty, G. A. (2005) De novo asymmetric synthesis of daumone via a palladium-catalyzed glycosylation, *Org. Lett. 7*, 3921–3924.
14. Makrigiorgos, G. M. (1997) Detection of lipid peroxidation on erythrocytes using the excimer-forming property of a lipophilic BODIPY fluorescent dye, *J. Biochem. Biophys. Methods 35*, 23–35.
15. Bargmann, C. I. (2006) Chemosensation in *C. elegans*, *WormBook 25*, 1–29.
16. Kawano, T., Katoka, N., Abe, S., Ohtani, M., Honda, Y., Honda, S., and Kimura, Y. (2005) Lifespan extending activity of substance secreted by the nematode *Caenorhabditis elegans* that include the dauer-inducing pheromone, *Biosci., Biotechnol., Biochem. 69*, 2479–2481.
17. Yoon, Y.-A., Kim, H., Lim, Y., and Shim, Y.-H. (2006) Relationships between the larval growth inhibition of *Caenorhabditis elegans* by apigenin derivatives and their structures, *Arch. Pharm. Res. 29*, 582–586.
18. Sato, S., Akiya, T., Nishizawa, H., and Suzuki, T. (2006) Total synthesis of three naturally occurring 6,8-di-C-glycosylflavonoids: phloretin, naringenin, and apigenin bis-C-beta-D-glucosides, *Carbohydr. Res. 341*, 964–970.
19. Bischof, L. J., Huffman, D. L., and Aroian, R. V. (2006) Assays for toxicity studies in *C. elegans* with Bt crystal proteins, *Methods Mol. Biol. 351*, 139–154.
20. Butcher, R. A., Fujita, M., Schroeder, F. C., and Clardy, J. (2007) Small-molecule pheromones that control dauer development in *Caenorhabditis elegans*, *Nat. Chem. Biol. 3*, 420–422.
21. Hedgecock, E. M., Thomson, J. N., and Culotti, J. G. (1986) Mutant sensory cilia in the nematode *Caenorhabditis elegans*, *Dev. Biol. 117*, 456–487.
22. Bell, L. R., Stone, S., Yochem, J., Shaw, J. E., and Herman, R. K. (2006) The molecular identities of the *Caenorhabditis elegans* intraflagellar transport genes *dyf*-6, *daf*-10 and *osm*-1, *Genetics 173*, 1275–1286.
23. Swoboda, P., Adler, H. T., and Thomas, J. H. (2000) The RFX-type transcription factor DAF-19 regulates sensory neuron cilium formation in *C. elegans*, *Mol. Cell 5*, 411–421.
24. Collins, T. J. (2007) ImageJ for microscopy, *Biotechniques 43*, 25–30.